

Electronic Supplementary Information

Enhancing room-temperature phosphorescence via intermolecular charge transfer in dopant-matrix systems

Xinjian Deng,^{a,b} Ju Huang,^{a,b} Guangming Wang,^b Jiuyang Li,^b Xun Li,^b Chuanhu Lei,^{*a} and Kaka Zhang^{*b}

^a. Department of Chemistry, College of Science, Shanghai University, Shanghai 200444, China;

^b. Key Laboratory of Synthetic and Self-Assembly Chemistry for Organic Functional Molecules, Shanghai Institute of Organic Chemistry, University of Chinese Academy of Sciences, Chinese Academy of Sciences, 345 Lingling Road, Shanghai 200032, People's Republic of China.

Email: chlei@shu.edu.cn; zhangkaka@sioc.ac.cn

Physical measurements and instrumentation

UV-Vis absorption spectra were recorded on a Techcomp UV1050 UV-vis spectrophotometer. The steady-state and delayed emission spectra were collected by Hitachi FL-4700 fluorescence spectrometer equipped with chopping systems; the delayed emission spectra were obtained with a delay time of approximately 1 ms. The excited state decay profiles in millisecond to second region were collected by Hitachi FL-4700 fluorescence spectrometer equipped with chopping systems. Photoluminescence quantum yield was measured by a Hamamatsu absolute PL quantum yield measurement system based on a standard protocol (*Adv. Mater.* **1997**, *9*, 230). Photographs and videos were captured by Honor 20 camera. Before the capture, samples were irradiated by a 365 nm UV lamp (5 W) for approximately 5 s at a distance of approximately 15 cm.

Materials

4-Aminobenzophenone (ABP) was purchased from Macklin and purified by recrystallization. Methyltriphenylphosphonium chloride (MTPPC) was purchased from Bidepharm and purified by chromatography and recrystallization.

Preparation of ABP-MTPPC afterglow materials

Firstly, MTPPC and ABP at a certain weight ratio were added to an agate mortar. Then a few drops of dichloromethane were added to facilitate the mixing process for dichloromethane can dissolve both MTPPC and ABP. After grinding and dichloromethane evaporation, the solid mixture of MTPPC and ABP that exhibited greenish afterglow was obtained. Materials of different ABP doping concentrations were prepared by the same method, whereas high concentration doping (>20 wt%) resulted in syrupy yellow mixture which did not exhibit room temperature afterglow.



Figure S1. Photographs of ABP-MTPPC-0.1% powder in a mortar showing intense afterglow under daylight.

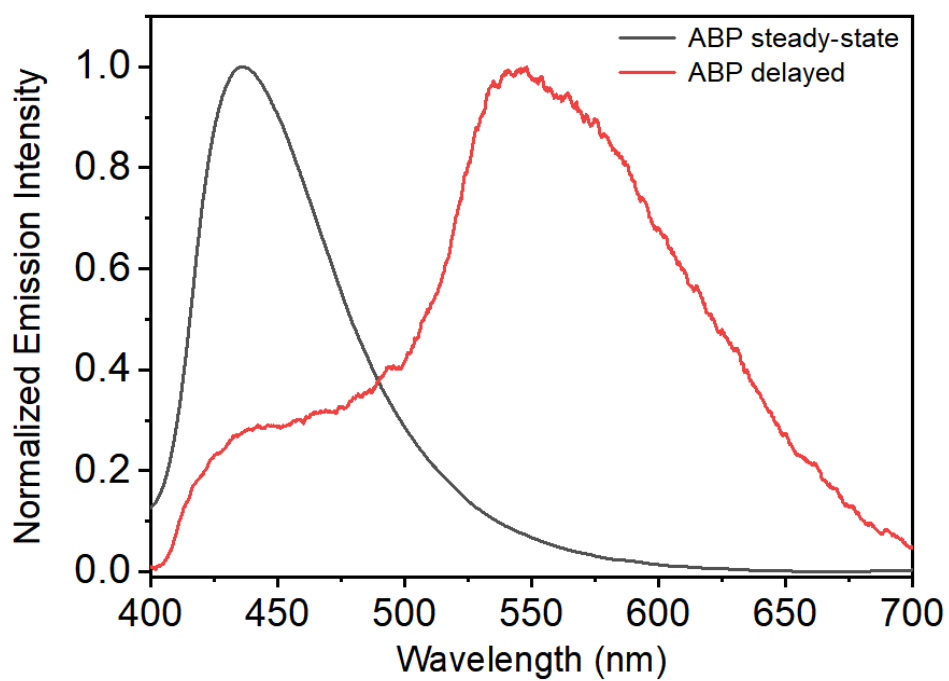


Figure S2. Steady-state and delayed spectra of ABP. Delayed emission of ABP powders is very weak ($\lambda_{\text{ex}} = 365 \text{ nm}$).

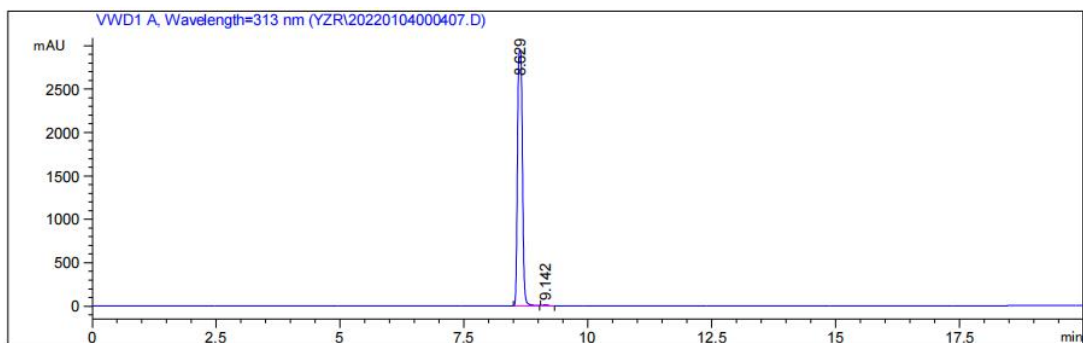


Figure S3. HPLC profile of ABP monitored at 313 nm by UV detector. It has been reported that impurity mechanism can lead to the emergence of significant afterglow in organic systems. In the present study, it is found that the increase of ABP doping concentration from 0.01% to 0.1% lead to enhancement of organic afterglow brightness. One may reason that there may be impurity in ABP, and the interaction of the impurity and MTPPC may give rise to significant organic afterglow. In the present study, the ABP compounds were carefully purified by recrystallization, and the high purity of the obtained ABP has been confirmed by HPLC measurement. Therefore, the impurity mechanism can be rule out in the present study.

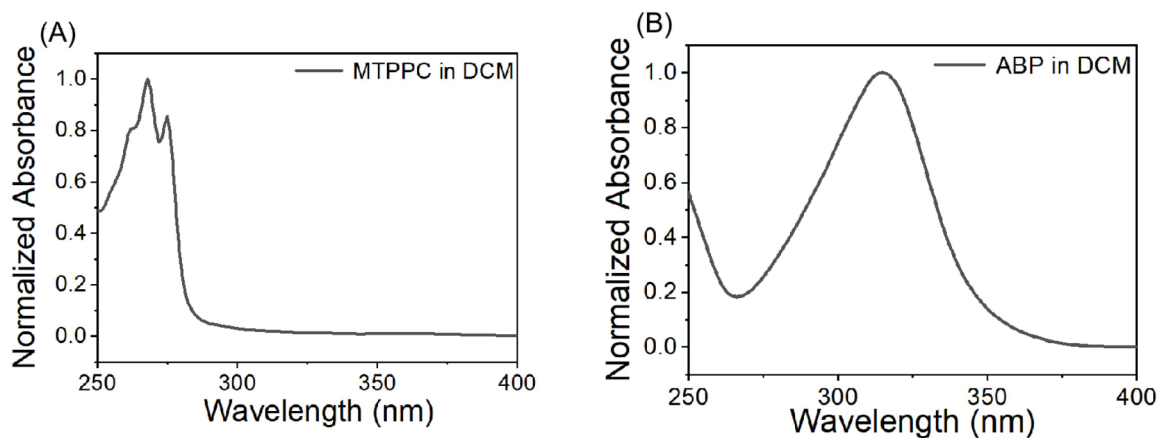


Figure S4. UV-vis absorption spectra of (A) MTPPC and (B) ABP in dichloromethane (DCM).

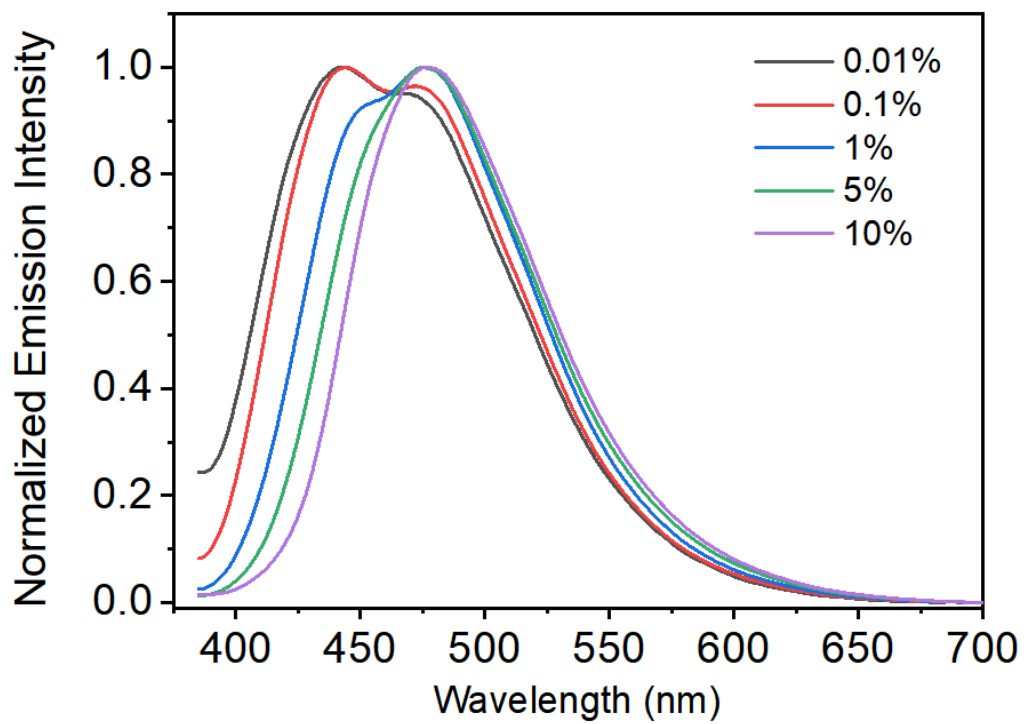


Figure S5. Steady-state spectra of ABP-MTPPC at different ABP doping concentrations ($\lambda_{\text{ex}} = 365$ nm).

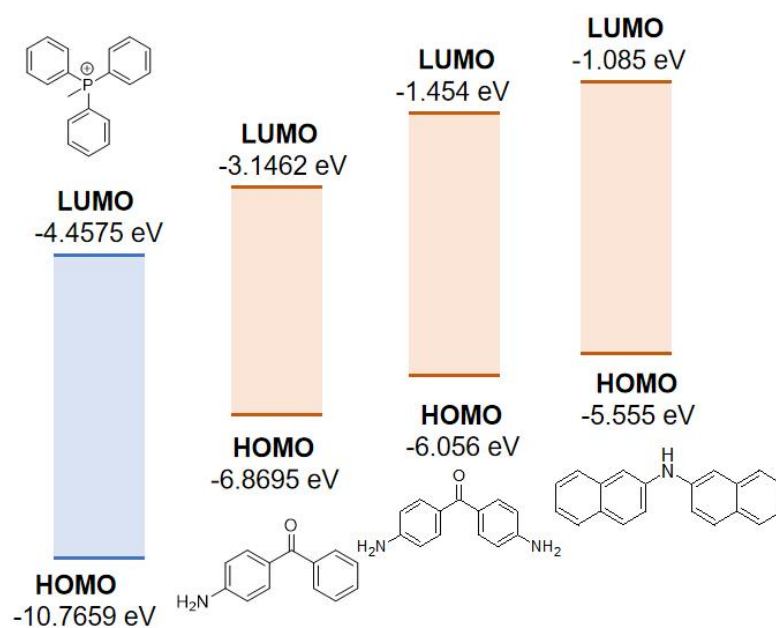


Figure S6. The HOMO and LUMO levels of ABP, 4,4'-diaminobenzophenone, 2,2-dinaphthylamine and MTPPC in MTPPC solid environment. To investigate the electronic properties of ABP and MTPPC embedded in the MTPPC solid environment, the QM/MM model was built from the single-crystal structure of MTPPC. The HOMO and LUMO levels of ABP and MTPPC in MTPPC solid environment have been estimated from TD-DFT calculation on Gaussian 16 program with PBE0 functional and 6-311G(d,p) basis set. The HOMO (-6.87 eV) and LUMO (-3.15 eV) levels of ABP are respectively higher than the HOMO (-10.77 eV) and LUMO (-4.46 eV) levels of MTPPC. Such HOMO/LUMO allows the formation of intermolecular charge transfer complexes between ABP (donor) and MTPPC (acceptor). Moreover, the red-shifted UV-vis absorption and steady-state emission spectra of ABP-MTPPC powders compared to those of ABP alone and MTPPC alone indicate the formation of intermolecular charge transfer complexes between ABP (donor) and MTPPC (acceptor). The ^1CT states (emission maxima at 472 nm, 2.63 eV) of ABP-MTPPC are slightly higher than the T_1 states (emission maxima at 488 nm, 2.54 eV) of MTPPC. On the basis of these, we propose that the $^1\text{CT}/^3\text{CT}$ states of ABP-MTPPC mediate the population of the T_1 states of MTPPC salts as shown in Scheme 2. For ^1CT to salt's T_1 transition, according to El-Sayed rule, ISC transition between excited states of different natures can be partially allowed and thus speed up, while the transition from ^3CT to salt's T_1 is spin-allowed; this is our understanding on the mechanism of the present two-component organic afterglow system with the involvement of intermolecular charge transfer. The HOMO and LUMO levels of 4,4'-diaminobenzophenone and 2,2-dinaphthylamine have also been calculated through the same procedures to those of ABP. It is found that the gap between 4,4'-diaminobenzophenone's HOMO and MTPPC's LUMO (1.60 eV) and the gap between 2,2-dinaphthylamine's HOMO and MTPPC's LUMO (1.10 eV) are much smaller than those in the case of ABP-MTPPC (2.41 eV). Such small HOMO-LUMO gaps give low $^1\text{CT}/^3\text{CT}$ energy levels in 4,4'-diaminobenzophenone-MTPPC and 2,2-dinaphthylamine-MTPPC systems, which would inhibit the energy transfer from CT states to MTPPC's T_1 states (estimated from phosphorescence maxima at 488 nm, 2.54 eV). As a result, insignificant organic afterglow has been observed in 4,4'-diaminobenzophenone-MTPPC and 2,2-dinaphthylamine-MTPPC systems.

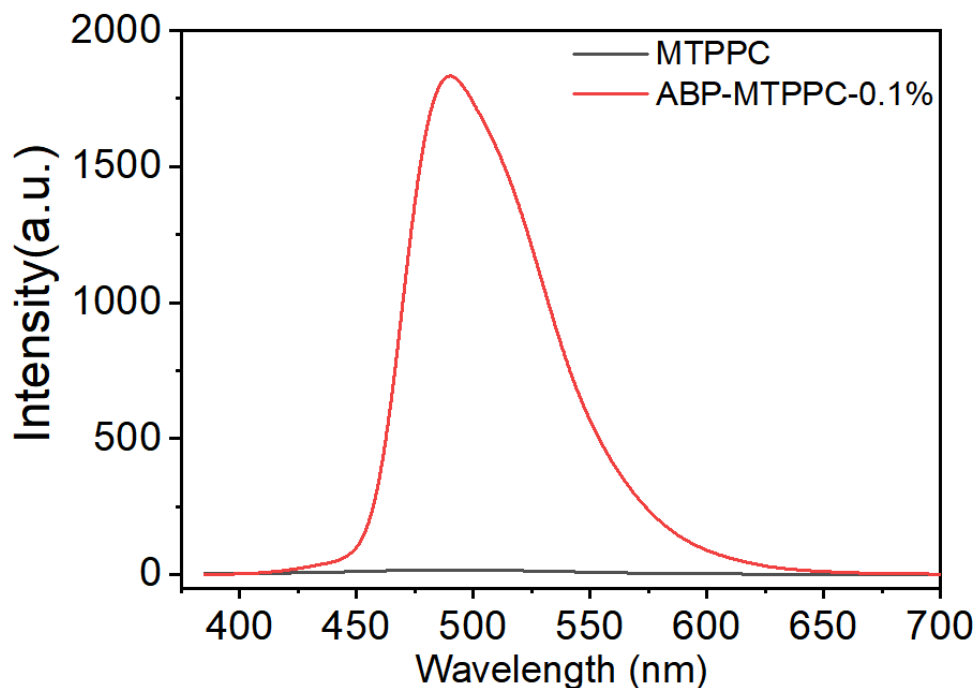


Figure S7. Delayed emission spectra of MTPPC and ABP-MTPPC-0.1% that show great enhancement of emission intensity after ABP doping ($\lambda_{\text{ex}}=365$ nm).

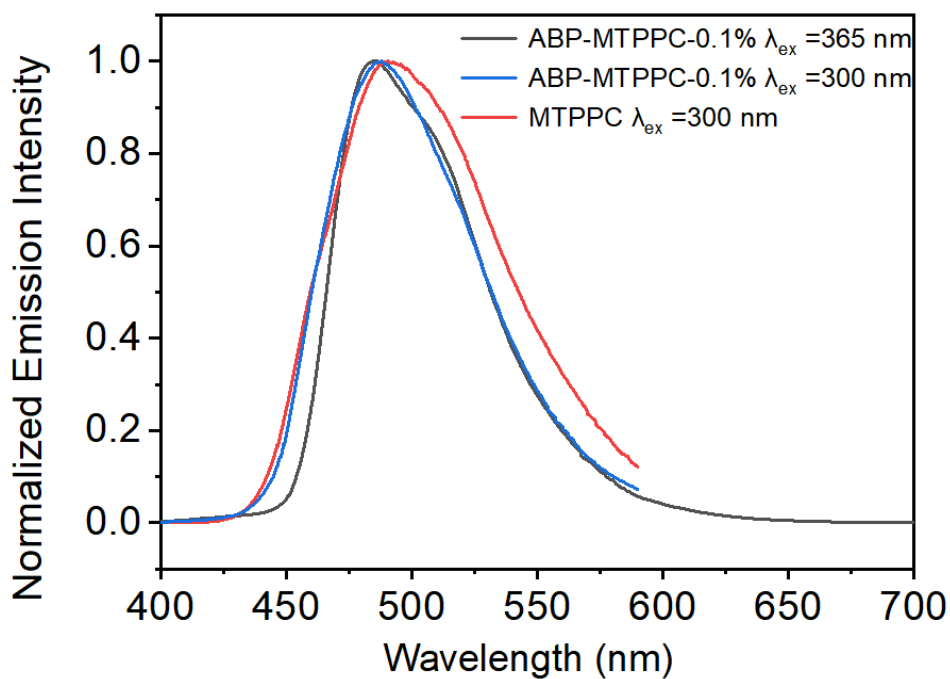


Figure S8. Delayed emission spectra of ABP-MTPPC-0.1% ($\lambda_{\text{ex}} = 365$ nm), ABP-MTPPC-0.1% ($\lambda_{\text{ex}} = 300$ nm) and MTPPC ($\lambda_{\text{ex}} = 300$ nm), which suggest the same origin of afterglow from T_1 energy level of MTPPC (emission peak at ~ 490 nm).

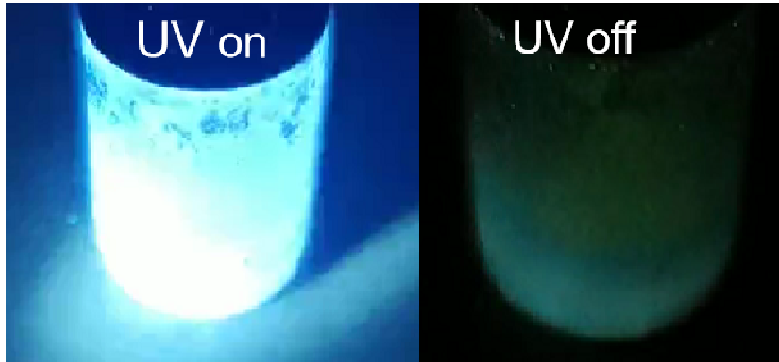


Figure S9. Photographs of purified MTPPC in dichloromethane at 77 K under 365 nm UV light and after turning the light off.

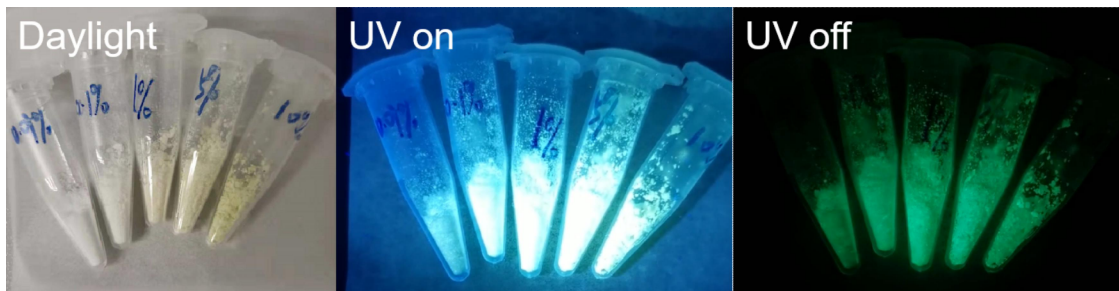


Figure S10. Photographs of ABP-MTPPC samples at different ABP doping concentrations under daylight, 365 nm UV light and after turning the light off (from left to right: 0.01 wt%, 0.1 wt%, 1 wt%, 5 wt%, and 10 wt%).

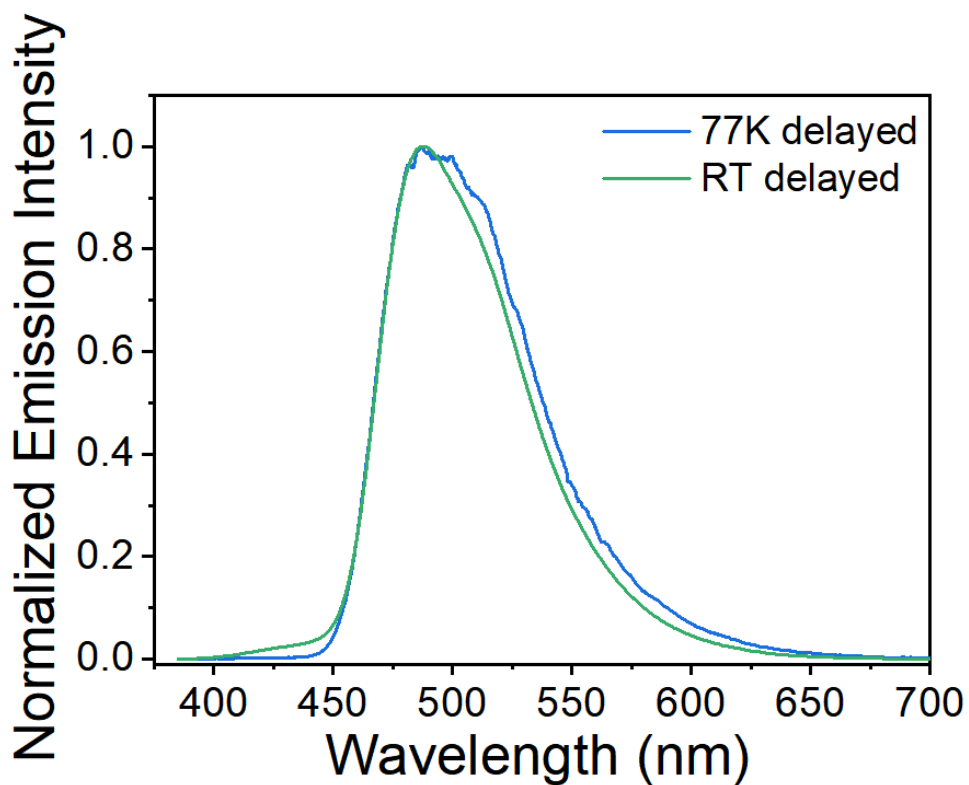


Figure S11. Delayed emission spectra of ABP-MTPPC-0.1% powders at 77 K and at room temperature. To rule out the TADF mechanism in the present study, delayed emission spectra of ABP-MTPPC-0.1% powders at 77 K have been collected to show very similar shape and maxima to those collected at room temperature. It is known that the TADF-type afterglow materials show red-shifted delayed emission spectra at 77 K when compared to those at room temperature. Therefore, the delayed emission bands of ABP-MTPPC-0.1% powders at room temperature are originated from RTP rather than TADF.

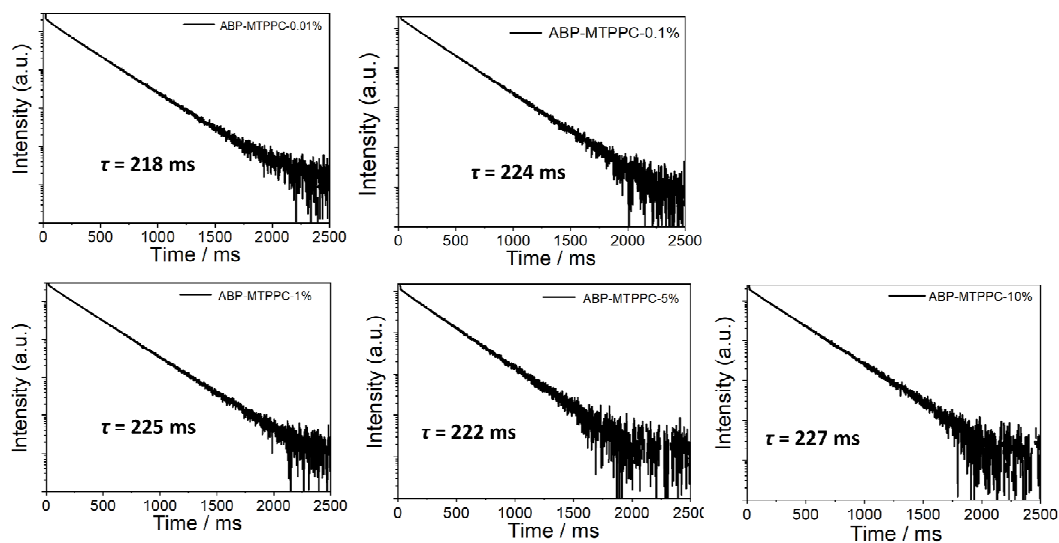


Figure S12. Emission decay curves of ABP-MTPPC powders (excited at 365 nm and monitored at 489 nm). The emission decay profiles have now been collected for ABP-MTPPC samples at doping concentrations 0.01%, 0.1%, 1%, 5% and 10%. The steady-state emission spectra of the samples at 5% and 10% doping concentrations exhibited more CT emission signals than the samples at 0.01%, 0.1% and 1% doping concentrations (Fig. S5). It is found that the afterglow brightness of samples at 0.1%, 1% and 5% is similar, while the afterglow emission lifetimes of these samples are also similar (Fig. 2D). It is noted that the rigidity of ABP-MTPPC samples at higher doping concentrations was reduced to a certain extent; ABP-MTPPC-50% samples are in a syrupy state. Therefore, the increase of ABP doping concentration can increase the population of triplet excited states but can also increase nonradiative decay of triplet excited states. Because of this, it is understandable that the ABP-MTPPC samples at 0.1%, 1% and 5% doping concentrations possess similar afterglow brightness and afterglow emission lifetimes.

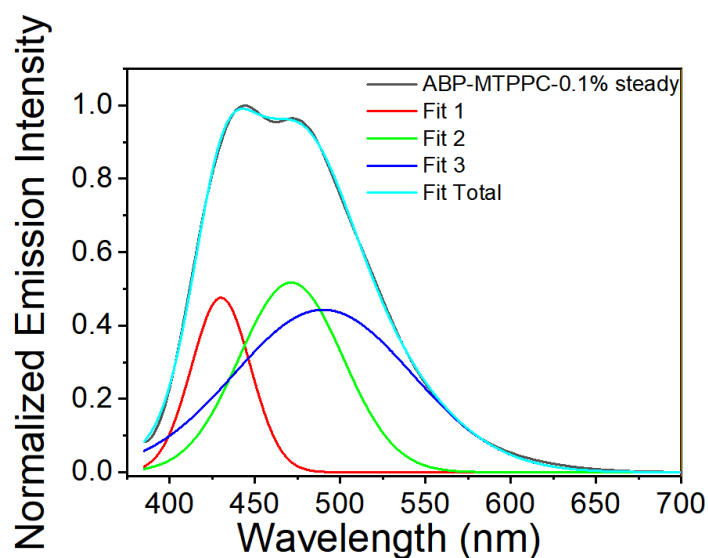


Figure S13. Peak separation of the steady-state emission spectra of ABP-MTPPC-0.1% powders. The blue curve with peak at 490 nm was attributed to RTP, which consists of 49.1% of the total emission spectra.

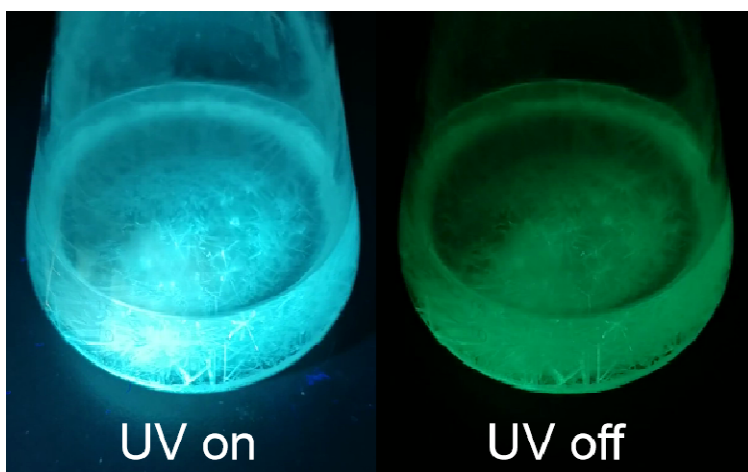


Figure S14. Photographs of ABP-MTPPC co-crystals under 365 nm UV light and after turning the light off. These co-crystals were obtained by recrystallization in dichloromethane (solvent) / n-hexane (non-solvent) system. The content of ABP in ABP-MTPPC crystals has been determined by UV-vis absorption measurement to be around 0.03%. Such a low doping concentration is enough for the emergence of organic afterglow but far less for crystal structural analyses. The structural information of co-crystals is very useful for the deep understanding of the emergence of afterglow in organic systems. It remains challenging for the present system to perform co-crystal analyses.

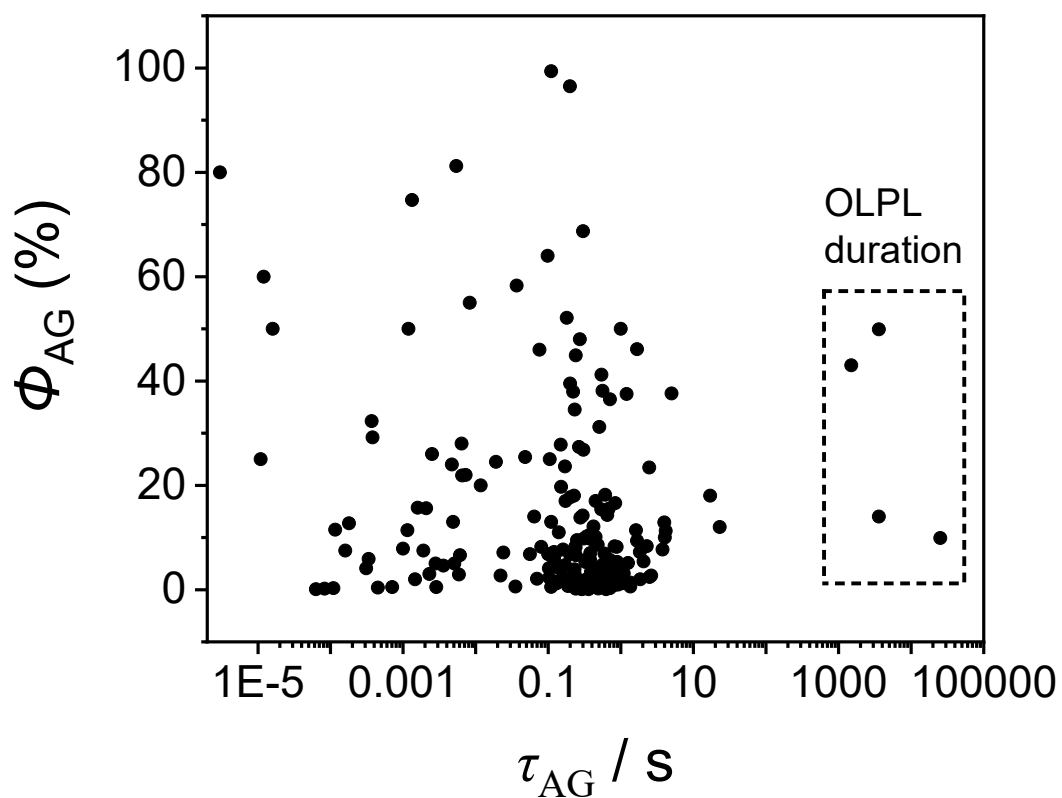


Figure S15. Afterglow quantum yields (Φ_{AG}) and afterglow emission lifetimes (τ_{AG}) of organic RTP and afterglow materials in the previously reported studies. For organic long-persistent luminescence (OLPL) system, afterglow duration is given rather than τ_{AG} (see the dashed box).

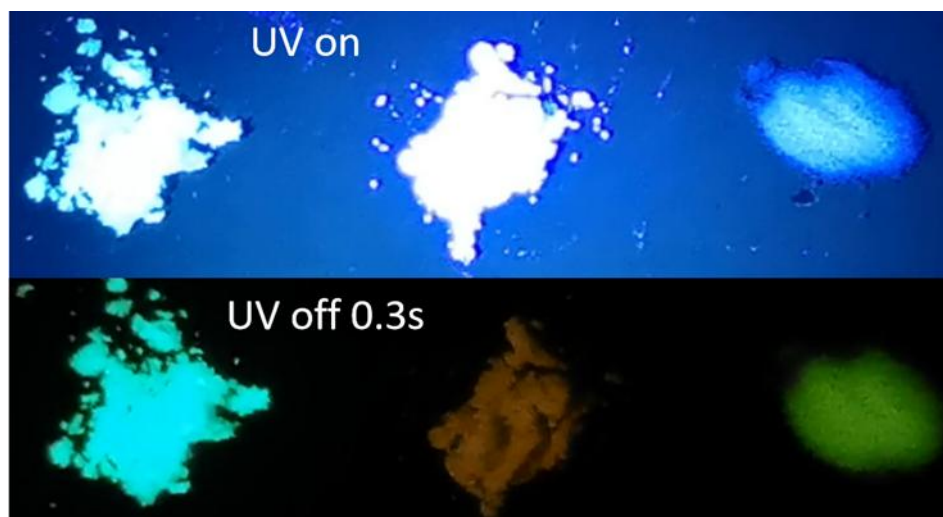


Figure S16. Afterglow brightness comparison between ABP-MTPPC-0.1% powders (left), commercial carbazole powders (middle) and *p*-phthalic acid powders (right).

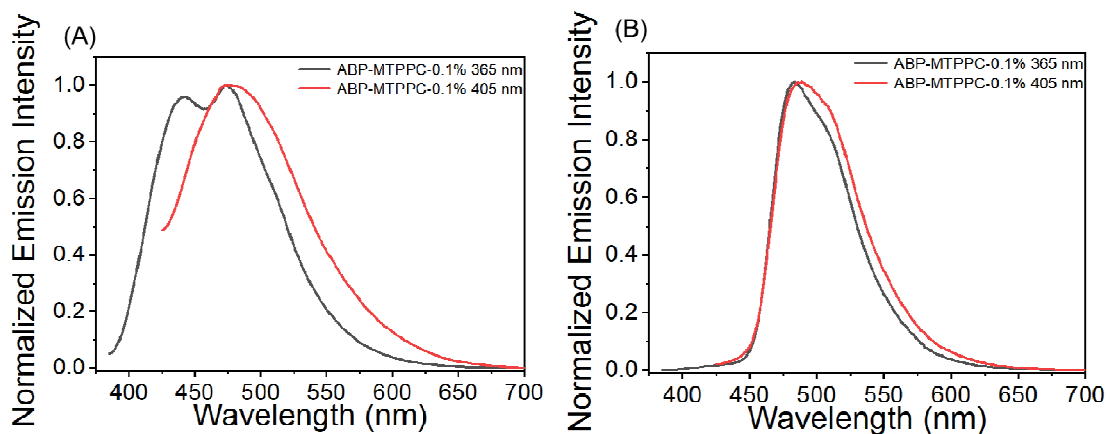
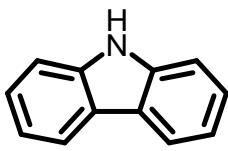
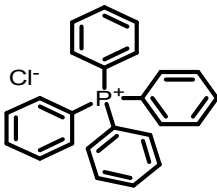
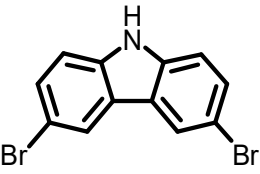
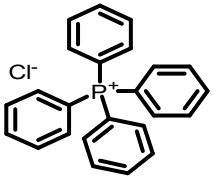
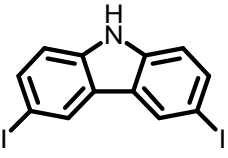
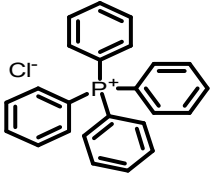
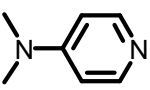
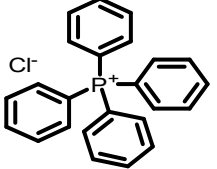
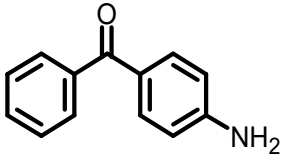
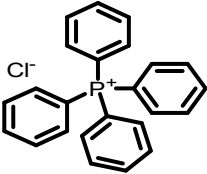
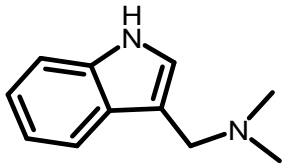
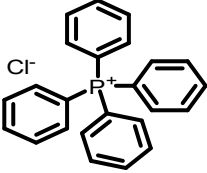
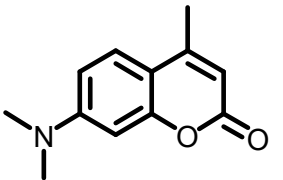
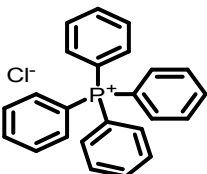
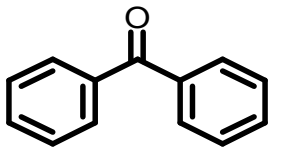
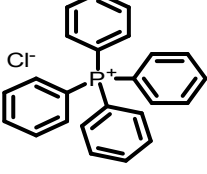
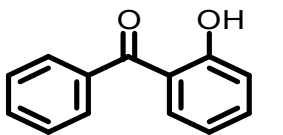
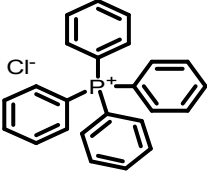
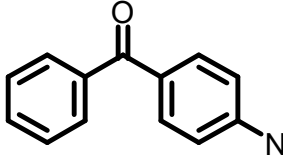
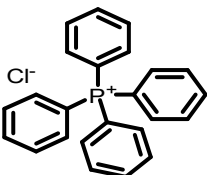
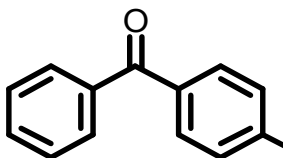
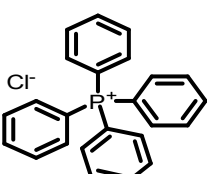
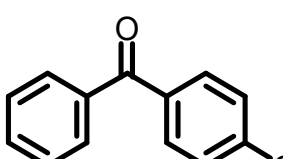
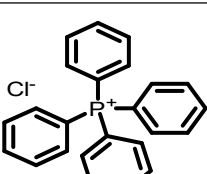
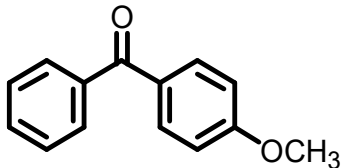
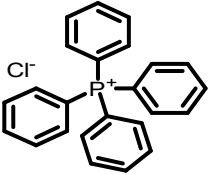
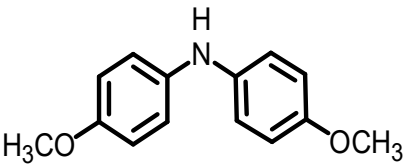
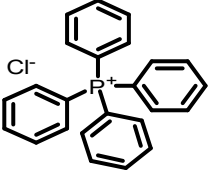
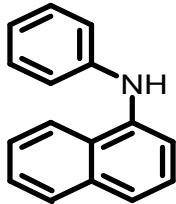
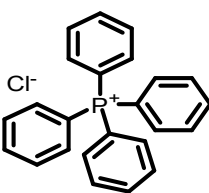
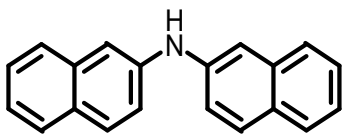
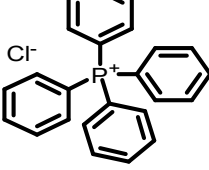
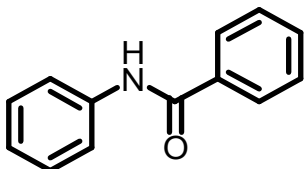
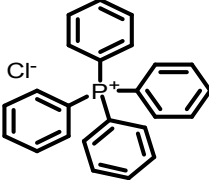
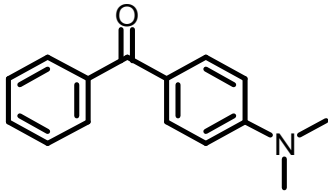
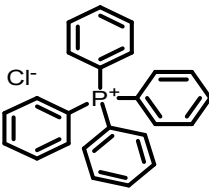
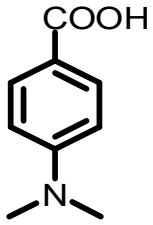
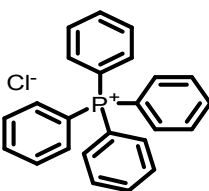
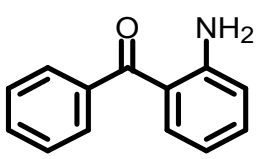
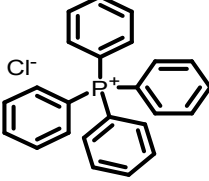


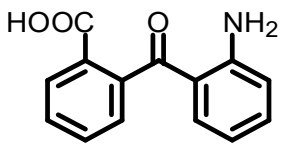
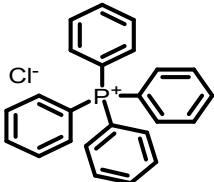
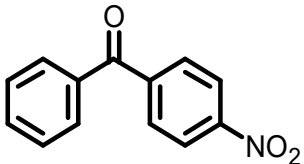
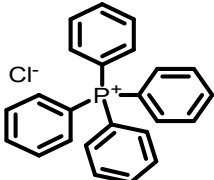
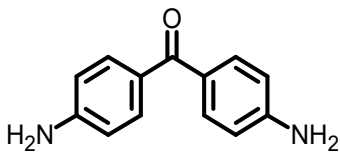
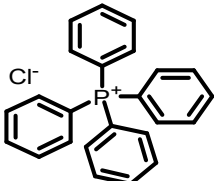
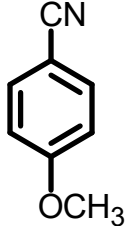
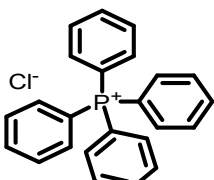

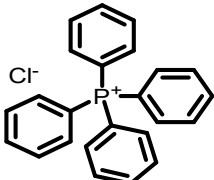
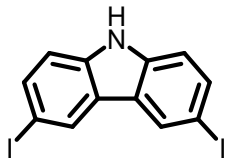
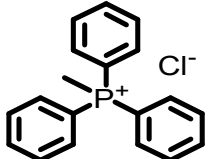
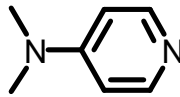
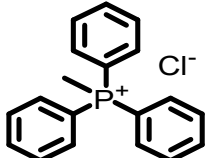
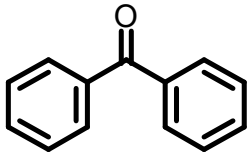
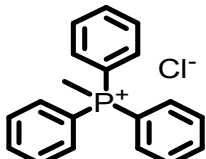
Figure S17. (A) Steady-state and (B) delayed spectra of ABP-MTPPC-0.1% excited at 365 nm and 405 nm.

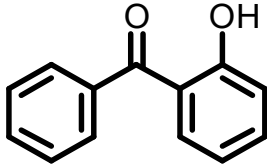
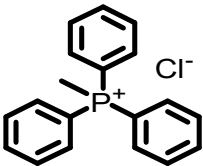
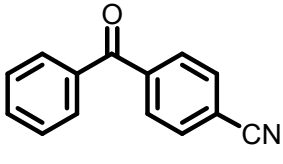
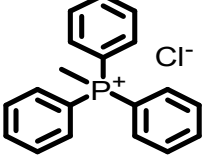
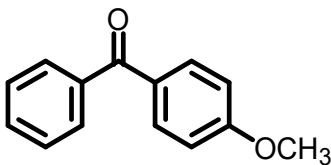
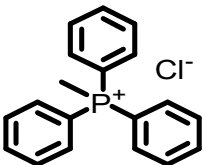
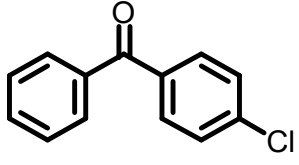
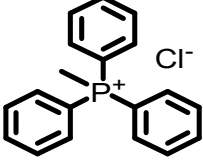
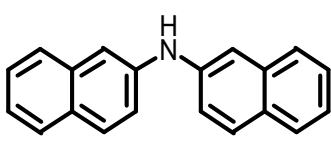
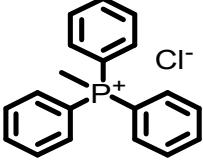
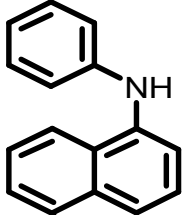
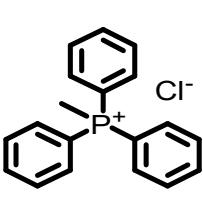
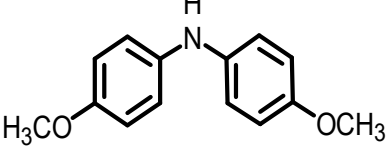
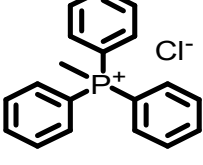
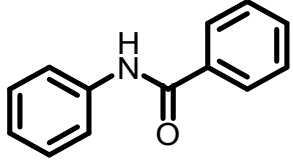
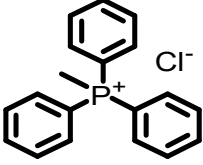
Table S1. Screening list of various dopants and matrices.

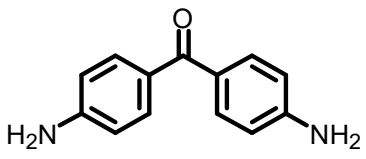
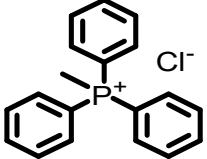
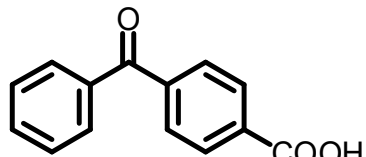
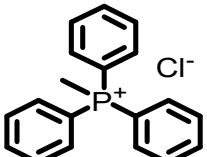
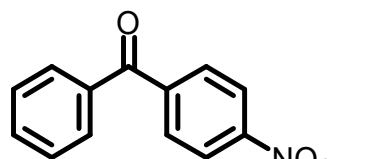
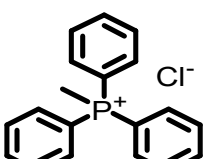
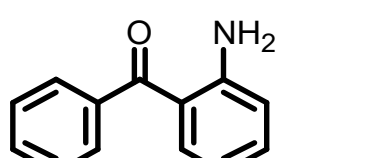
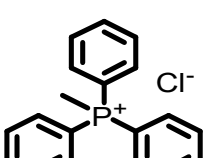
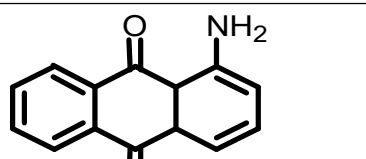
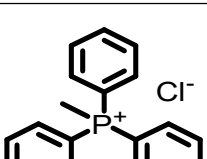
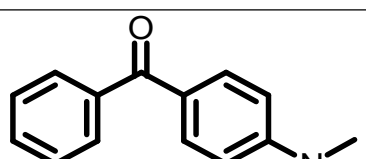
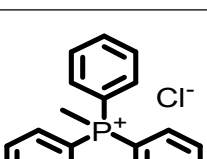
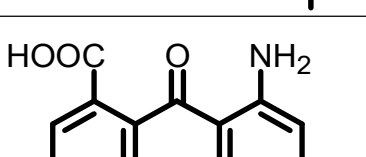
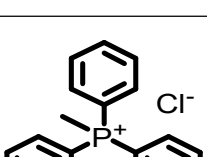
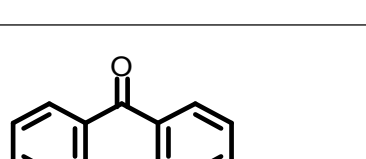
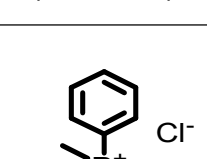
Dopants	Matrices	Afterglow
		Weak orange-yellow afterglow with duration of ~2s
		No afterglow
		No afterglow
		Weak green afterglow with duration of ~2s

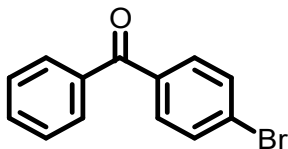
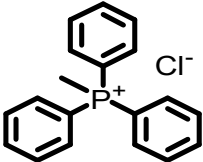
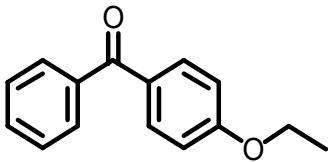
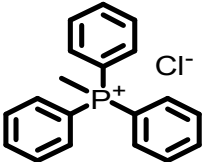
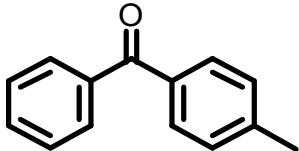
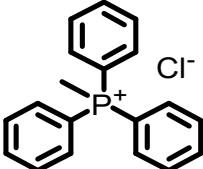
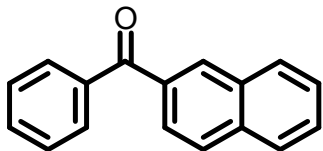
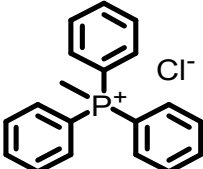
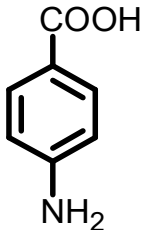
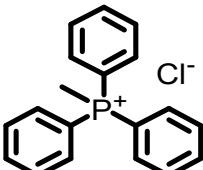
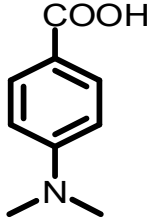
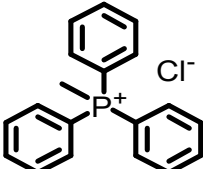
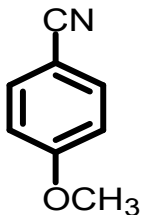
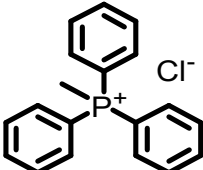
		No afterglow
		No afterglow
		Weak yellow afterglow with duration of ~5s
		Weak afterglow
		No afterglow
		No afterglow
		Weak yellow afterglow with duration of ~ 1s
		No afterglow


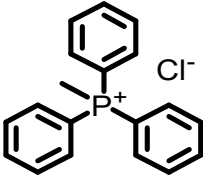
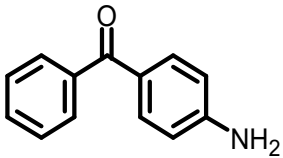
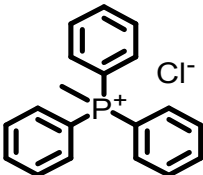
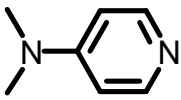
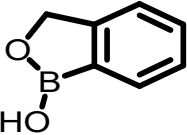
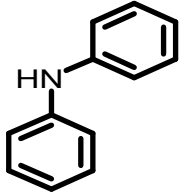
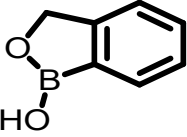
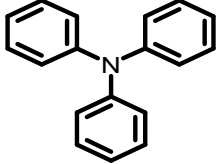
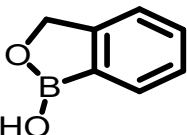
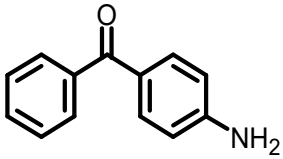
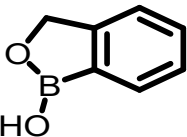
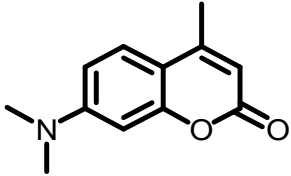
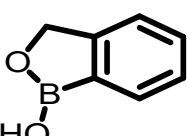
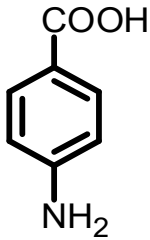
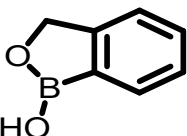
		Weak afterglow with duration of ~ 2s
		No afterglow
		Weak orange-yellow afterglow with duration of ~ 2s
		Weak yellowish green afterglow with duration of ~ 1s
		No afterglow
		No afterglow
		Weak afterglow with duration of ~ 2s
		No afterglow

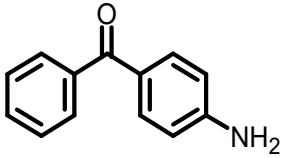
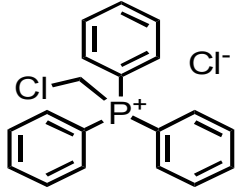
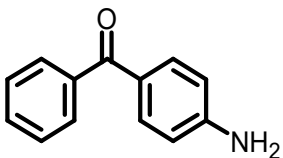
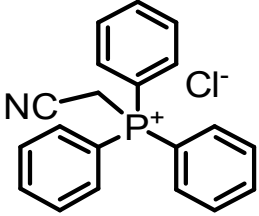
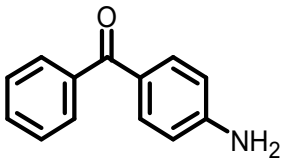
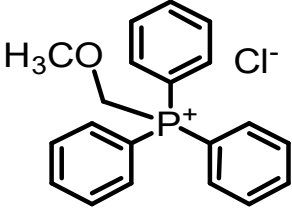
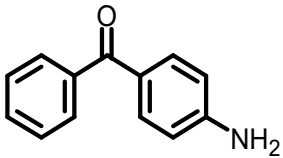
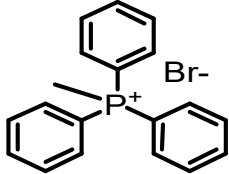
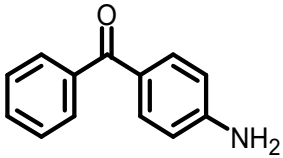
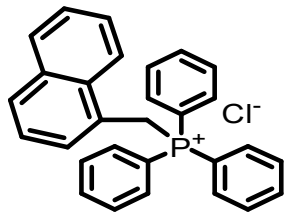
		No afterglow
		No afterglow
		No afterglow
		No afterglow
		Very short afterglow
		Weak green afterglow with duration of ~2s
		Weak green afterglow with duration of ~ 2s
		Weak green afterglow with duration of ~ 2s

		Weak green afterglow
		Weak green afterglow
		Weak green afterglow
		Yellow afterglow with duration of ~ 2s
		Weak yellowish green afterglow with duration of ~ 2s
		Weak orange-yellow afterglow with duration of ~2s
		No afterglow
		Weak yellowish green afterglow with duration of ~ 2s

		No afterglow
		Weak yellow afterglow with duration of ~ 2s
		Weak green afterglow with duration of ~ 2s
		No afterglow
		No afterglow
		Weak green afterglow with duration of ~ 3s
		No afterglow
		Weak yellowish green afterglow with duration of ~ 5s

		Weak yellow afterglow with duration of ~ 3s
		Weak afterglow
		Weak green afterglow with duration of ~ 2s
		Weak yellowish Green afterglow with duration of ~ 3s
		Weak green afterglow with duration of ~ 3s
		Weak blue afterglow with duration of ~ 3s
		Weak green afterglow with duration of ~ 3s

		Weak green afterglow
		Very bright green afterglow with duration of ~ 2s
		No afterglow
		No afterglow
		No afterglow
		No afterglow
		No afterglow
		No afterglow

		No afterglow
		Weak afterglow
		No afterglow
		No afterglow
		No afterglow

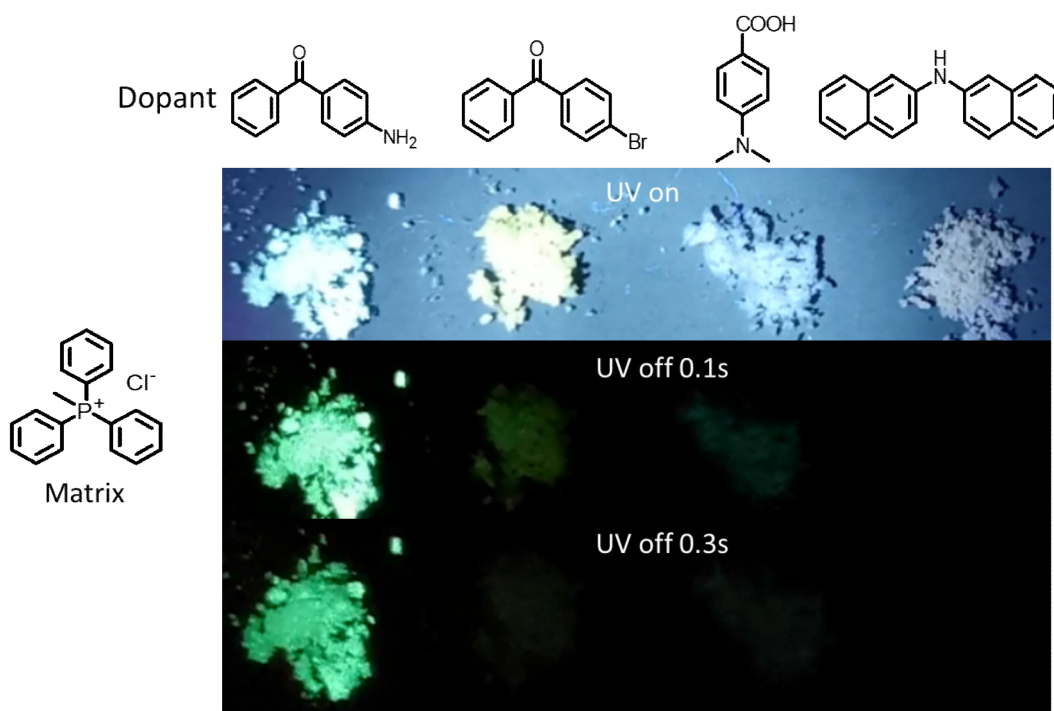


Figure S18. Photographs of some dopant-matrix samples during screening. The dopant-matrix samples showed weak blue, yellow and orange afterglow. The afterglow properties of these samples are very weak and with short duration. The weak blue afterglow should be originated from dopant's T_1 with the protection of rigid MTPPC environment. The weak yellow and orange afterglow can be attributed to the T_1 states of dopants with large conjugation. Because the afterglow is very weak, we didn't perform further study on these dopant-matrix samples. As discussed in the main text, because the emergence of intense organic afterglow requires two conditions: (a) the formation of intermolecular charge transfer complexes between dopants and matrices, (b) the slightly higher ${}^1CT/{}^3CT$ states of dopant-matrix complexes than T_1 states of matrices, the dopant-matrix combination in Table S1 (except in the case of ABP-MTPPC) didn't lead to significant organic afterglow under ambient conditions.